



## INVESTIGATION OF THE EFFECT OF EXTREME COLD TEMPERATURES ON THE IMPACT BEHAVIOR OF CFRP COMPOSITE SANDWICH PANELS: NUMERICAL SIMULATION DEVELOPMENT

Jean-St-Laurent, M<sup>1</sup>, Dano, M-L<sup>1\*</sup>, and Potvin, M-J<sup>2</sup>

<sup>1</sup> Department of Mechanical Engineering, Laval University, Québec, Canada

<sup>2</sup> Canadian Space Agency, St-Hubert, Canada

\* Marie-Laure Dano (marie-laure.dano@gmc.ulaval.ca)

### ABSTRACT

The effect of extreme cold temperatures on the low velocity impact behavior of carbon/epoxy woven sandwich panels with Nomex honeycomb core has been studied. Low velocity impact tests were performed at room temperature,  $-70^{\circ}\text{C}$ , and  $-150^{\circ}\text{C}$  under various impact conditions. Small effects of temperature are observed on the load-displacement curves, while there is an increase of damage induced for specimens impacted at cold temperatures. A finite element model to simulate the behavior of the sandwich panels was developed based on damage mechanics. The developed model is applied to the simulation of impact loadings at room temperature,  $-70^{\circ}\text{C}$ , and  $-150^{\circ}\text{C}$  and is validated with the results of the experimental tests. Overall, the model predicts well the behavior of the sandwich panel under impact loadings.

**KEYWORDS:** *Finite element analysis, damage mechanics, environmental effects, low velocity impact.*

### 1 INTRODUCTION

Carbon/epoxy composite sandwich panels with Nomex honeycomb core are considered for the fabrication of lunar exploration rovers. Their excellent mechanical and thermal properties, as well as their lightness, make them good candidates for space applications. On the moon, rovers will be exposed to extremely cold temperatures, especially near the permanent shadowed areas, which are nowadays the main areas of interest because of the presence of water. Moreover, on the moon, rovers will work on a rugged terrain with loose rocks and craters and they will have to do so with a limited knowledge of the real nature of the ground, due to the presence of lunar dust in suspension, as well as a thick layer of up to 30 cm of loose dust on the ground. Thus, impacts between a rover and its surroundings are a real possibility and are likely to occur at extreme cold temperatures. It is therefore essential to understand the effect of cold temperatures on the impact behavior of composite sandwich panels.

A few studies have looked at the effect of temperature on the impact behavior of composite sandwich panels (Elamin et al. 2018; Erickson et al., 2005; Sakly et al., 2016; Salehi-Khojin et al., 2005; Yang et al., 2015). However, amongst them, none has studied temperatures as low as  $-150^{\circ}\text{C}$  and none have studied sandwich panels with constituents fit for space applications, satisfying the stringent requirements in outgassing and compatibility of coefficients of thermal expansion. In order to have information on the behavior of carbon fiber composite structures in such a cold environment, studies on carbon fiber composite laminates are available (Gómez-del-Río et al., 2005; López-Puente et al., 2002; Sánchez-Sáez et al., 2006). Those studies show that there is an increase of damage at cold temperatures when testing between room

temperature and  $-150^{\circ}\text{C}$  and that the stacking sequences, as well as the fiber architecture, will influence the effect of temperature on the impact behavior.

Modelling of impact behavior of composite laminates and composite sandwich panels has received a lot of attention in past decades. Indeed, experimental testing is costly and time consuming, which makes the development of efficient numerical tools essential. However, most of the time, the developed model is only used at room temperature, with a few exceptions. Gómez-del-Rio et al. (2003) have performed impact simulations on carbon-epoxy laminates at RT,  $-20^{\circ}\text{C}$ , and  $-150^{\circ}\text{C}$ . The failure behavior of the composite was based on Hou criteria (Hou et al., 2000) and included four failure modes. Yang et al. (2015) developed a model to simulate impact loading at different temperatures on sandwich panels with composite skins and polymeric foam core. They used damage mechanics to model the failure of the composite.

The objective of the herein project is to study the effects of extreme cold temperatures on the impact behavior of composite sandwich panels for lunar exploration rovers. In order to do so, experimental impact tests were performed at room temperature,  $-70^{\circ}\text{C}$ , and  $-150^{\circ}\text{C}$ . A finite element model has also been developed to study impact loadings at those three temperatures. In this paper, a review of the tests performed is presented with an emphasis on the main results and conclusions. The numerical model developed is explained in details and the results of the numerical investigations are compared to the experimental ones for validation purposes.

## **2 MATERIAL**

The sandwich panel is made of plain weave carbon-epoxy composite skins and a Nomex honeycomb core and has the following stacking sequence:  $[(\pm 45)/(0/90)/(0/90)/(\pm 45)/\text{core}/(\pm 45)/(0/90)/(0/90)/(\pm 45)]$ . The resin is a 977-2 epoxy. The core is made of 4.76 mm regular hexagonal cells and has a density of  $48 \text{ kg/m}^3$ . The core is 12.7 mm thick and the total thickness of the panel is around 14.5 mm. All of the sandwich panel constituents were chosen because they fulfilled space application requirements.

## **3 IMPACT TESTS**

Since lunar exploration rovers are limited in terms of velocity, all the tests were performed at the same initial impact velocity of 1 m/s. In order to study a wide range of damage types and sizes, two hemispherical impactors with a 12.7 mm and a 25.4 mm diameter were used, combined with different impactor masses. For all the impact conditions, five tests were performed at room temperature,  $-70^{\circ}\text{C}$ , and  $-150^{\circ}\text{C}$ .

Impact tests were performed on an Instron 9340 drop tower. For the tests at  $-70^{\circ}\text{C}$  and  $-150^{\circ}\text{C}$ , a modified environmental chamber cooled with liquid nitrogen was used. During testing, specimens were clamped on a steel support with an inner diameter of 76.2 mm. An anti-rebound system was used to prevent a second impact on the specimens.

Prior to every test, specimens were dried in an oven to remove moisture. For the tests at cold temperatures, once the desired temperature was reached, specimens were kept at that temperature for 15 minutes before the beginning of the test.

## **4 NUMERICAL SIMULATIONS**

### **4.1 General Model Description**

Impact simulations are performed with Abaqus/explicit. A quarter of the specimen is modelled with the adequate symmetry and boundary conditions. The impactor is modelled as a rigid body. Each ply of the composite skin is modelled as a different part with one element through its thickness. C3D8R solid elements are used. The cellular geometry of the core is modelled with S4R shell elements. A perfect bond is assumed between the composite plies and between the composite skins and the Nomex core. An initial velocity is applied to the impactor. The effect of gravity is included in the model.

## 4.2 Composite Material Behavior

The composite material model is based on damage mechanics. Three damage variables are used. Two are associated with the failure behavior in the warp and weft directions ( $d_{11}$  and  $d_{22}$ ), and one is associated with the in-plane shear behavior ( $d_{12}$ ).

### 4.2.1 Tensile and Compressive Behavior in the Warp and Weft Directions

In the warp and weft directions, the damage variables characterise the post-failure behavior. The initiation of failure is predicted with the maximum strain criteria. Once failure is initiated, the stress evolves linearly down to zero (Figure 1). Two independent damage variables are used for the tensile and compressive behaviors. They follow the same evolution law with different parameters.

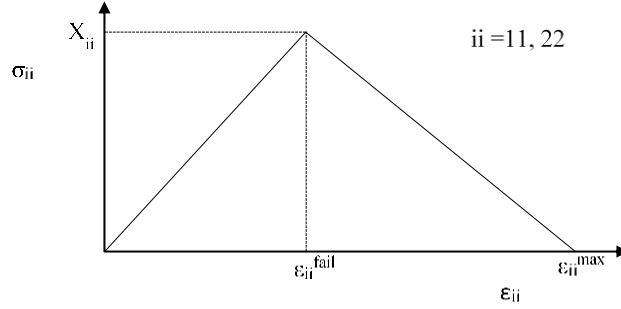


Figure 1. Stress-strain relationship in the warp and weft directions.

The evolution of the damage variables is given by the following expression:

$$d_{ii} = \begin{cases} |\varepsilon_{ii}| < \varepsilon_{ii}^{fail}, & 0 \\ |\varepsilon_{ii}| \geq \varepsilon_{ii}^{fail}, & \frac{\varepsilon_{ii}^{max}}{\varepsilon_{ii}^{max} - \varepsilon_{ii}^{fail}} \left( 1 - \frac{\varepsilon_{ii}^{fail}}{\varepsilon_{ii}} \right) \\ d_{ii} \geq d_{ii}^{max}, & d_{ii}^{max} \end{cases}, \quad (ii = 11, 22) \quad (1)$$

where,  $\varepsilon_{ii}^{fail}$  is the strain at the initiation of failure, and  $\varepsilon_{ii}^{max}$  is the maximum strain associated with the complete state of failure of the element. The value of  $\varepsilon_{ii}^{max}$  is based on the Bažant and Oh (1983) band criteria which relies on the principle that failure is restricted to a band of elements. In order to maintain the same energy dissipation at failure for any size of element, the maximum strain is function of the critical fracture energy per unit of area ( $G_c$ ) and a characteristic length of the element ( $l_c$ ):

$$\varepsilon_{ii}^{max} = \frac{2G_c}{X_{ii}l_c}, \quad (ii = 11, 22) \quad (2)$$

The introduction of the characteristic length allows to alleviate mesh dependency. The characteristic length used in this model is given by the following expression (Lapczyk and Hurtado, 2007):

$$l_c = \sqrt{A_{IP}} \quad (3)$$

where  $A_{IP}$  is the in-plane area corresponding to an integration point. The characteristic length corresponds to the length of a square element in its principal directions.

#### 4.2.2 In-Plane Shear Behavior

The in-plane shear behavior is characterised by important non-linearities and by inelastic strains. In order to take those two phenomena into account, the model introduces the use of a damage variable combined with a plasticity model (Hochard et al., 2001).

The evolution of the damage variable is function of thermodynamic forces:

$$Y_{ii} = \frac{\sigma_{ii}^2}{2E_i(1-d_i)^2} \quad , \quad (ii = 11, 22) \quad \text{and} \quad Y_{12} = \frac{\sigma_{12}^2}{2G_{12}(1-d_{12})^2} \quad (4)$$

An equivalent thermodynamic force is defined to take into account the effect of tensile strength in the warp and weft directions on the development of shear damage:

$$Y_{eq} = \alpha(Y_{11})_+ + \alpha(Y_{22})_+ + Y_{12} \quad \text{and} \quad \bar{Y}_{eq}(t) = \text{Sup}_{\tau \leq t}(Y_{eq}(\tau)) \quad (5)$$

where  $\alpha$  is a coupling parameter. The evolution of the damage variable  $d_{12}$  is given by:

$$\text{if } \bar{Y}_{eq} > Y_0, \quad d_{12} = \frac{\sqrt{\bar{Y}_{eq} - \sqrt{Y_0}}}{\sqrt{Y_C - \sqrt{Y_0}}} \quad (6)$$

where  $Y_0$  is the thermodynamic force that initiates the damage evolution and  $Y_C$  is the critical thermodynamic force. They characterise the evolution of damage before the initiation of failure. The plastic function is given by the following expression:

$$f = \sqrt{\left(\frac{\sigma_{12}}{(1-d_{12})}\right)^2} - R(p) - \sigma_y \quad (7)$$

$\sigma_y$  is the initiation plasticity stress.  $R(p)$  is the hardening law defined by:

$$R(p) = Cp^k \quad (8)$$

where  $p$  is the cumulated plastic strain and  $C$  and  $k$  are the parameters of the hardening law.

The in-plane shear failure initiation is also predicted with the maximum strain criteria. Once failure is predicted, a new damage evolution law is introduced and plasticity is not taken into consideration anymore. The in-plane shear stress evolves linearly to zero (Figure 2) in a similar fashion as in the warp and weft directions. The evolution of the shear damage variable after failure initiation is given by the following expressions:

$$d_{12} = d_{12}^{I,max} + d_{12}^{II} \quad (9)$$

$$d_{12}^{II} = (1 - d_{12}^{I,max}) \left( \frac{\varepsilon_{12}^{max} - \varepsilon_{12}^{P,max}}{\varepsilon_{12}^{max} - \varepsilon_{12}^{fail}} \left( 1 - \frac{\varepsilon_{12}^{fail} - \varepsilon_{12}^{P,max}}{\varepsilon_{12}^e} \right) \right)$$

- $d_{12}^{I,max}$  : is the maximum value of the damage variable before the initiation of failure.
- $\varepsilon_{12}^{P,Max}$  is the maximum value of the plastic strain before the initiation of failure.
- $\varepsilon_{12}^e$  is the elastic strain.

The maximum in-plane shear strain definition is also based on the Bažant and Oh (1983) band criteria:

$$\varepsilon_{12}^{max} = \left( \frac{G_{12,C}}{2 l_c} - A_1 \right) \frac{2}{X_{12}} + \varepsilon_{12}^{fail} \quad (10)$$

where  $A_1$  is the area under the stress-strain curve before the initiation of failure (Figure 2).  $A_1$  is evaluated numerically.  $G_{12,C}$  is the in-plane shear critical fracture energy per unit of area.

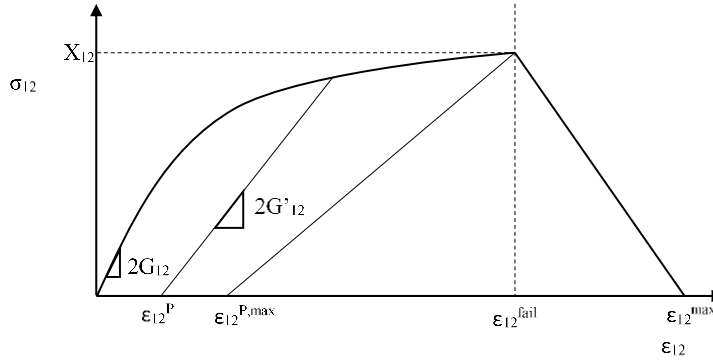


Figure 2. In-plane stress-strain shear relationship.

#### 4.2.3 Delamination

Delamination is an important failure mode for composite structures under impact loading. In the model, a quadratic failure criterion based on the work of Brewer and Lagace (1988) is used to predict delaminations:

$$\left( \frac{\langle \sigma_{33} \rangle_+}{X_{33}} \right)^2 + \left( \frac{\sigma_{23}}{X_{23}} \right)^2 + \left( \frac{\sigma_{13}}{X_{23}} \right)^2 = 1 \quad (11)$$

where  $X_{33}$ ,  $X_{13}$  and  $X_{23}$  represent respectively the out-of-plane tensile strength and out-of-plane shear strengths. The criterion is combined with the degradation of out-of-plane elastic properties.

#### 4.2.4 Element Deletion

Element deletion is added to the composite material model to remove failed elements from the simulation. An element is deleted from the simulation if either  $d_{11}$  or  $d_{22}$  reaches the value of  $d_{ii}^{max}$ .

#### 4.2.5 Parameter Identification

The in-plane elastic and failure properties in tension and compression are obtained at room temperature and cold temperatures from experimental investigations (Jean-St-Laurent et al., 2018). The tensile strength decreases at cold temperature, while the compressive stress increases. As for the elastic modulus, it remains the same. The critical fracture energy per unit of area is estimated based on the literature (Gauthier, 2010) and numerical simulations. At cold temperature, the model states that the critical fracture energy per unit of area varies proportionally with the ultimate tensile or compressive stresses.

The elastic and non-linear shear properties are also obtained from experimental investigations. Monotonic and cyclic shear tests were performed at room temperature,  $-70^\circ\text{C}$ , and  $-150^\circ\text{C}$ . As temperature decreases, the shear behavior becomes more fragile. There is an increase of the elastic shear modulus and a decrease of the shear strain at failure. The amount of inelastic strain also diminishes at cold temperature. The critical shear fracture energy per unit of area is obtained from the literature (Donadon et al., 2008; Gauthier, 2010). At cold temperature, the change in the critical shear fracture energy per unit of area is assumed to be proportional to the change in the area under the stress-strain curve before failure initiation ( $A_1$ ).

Out-of-plane elastic properties and failure properties are obtained from the literature (Turon et al., 2007) and the Composite Handbook (2012). The evolution of the out-of-plane shear properties at cold temperature is supposed to follow the evolution of the in-plane shear modulus at cold temperature. As for the effect of temperature, on the out-of-plane elastic modulus and ultimate stress, they are kept the same at cold temperature, due to the limited literature regarding that subject.

### 4.3 Nomex Honeycomb

The cellular geometry of the Nomex is modelled with each cell represented as a perfect hexagon. Nomex honeycomb core is made of Nomex paper dipped in phenolic resin. In the model, the paper and the phenolic resin are represented as one material with an isotropic elastic perfectly plastic behavior.

Out-of-plane compressive tests of the Nomex honeycomb were performed at room temperature, -70°C, and -150°C (Figure 3). The properties of the cell equivalent material ( $E$ ,  $\sigma_y$ ) are obtained by fitting the results of out-of-plane compressive test simulations and experimental results at all three temperatures. The properties obtained are then used for the simulations of impact loadings.

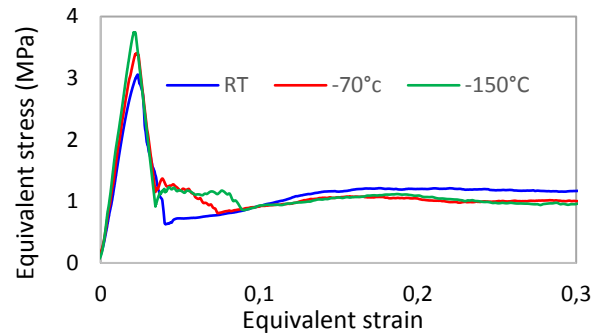


Figure 3. Equivalent out-of-plane compressive stress-strain curves for the Nomex honeycomb core at room temperature, -70°C, and -150°C.

## 5 RESULTS

Figure 4 presents the experimental load-displacement curves and the damaged cross sections for specimens impacted with the 12.7 mm impactor and a 5 kg mass at room temperature, -70°C, -150°C. As temperature decreases, the loads diminish while the maximum displacement increases. Important load drops are observed for specimens impacted at -150°C, an indication of load bearing capacity loss caused by important impact damages. Damage evaluation show that the damage induced increases for impact testing at cold temperature. The number of cracks is more important and the residual depth of indentation is larger. Those observations also apply to the other impact conditions. However, the effect of temperature is more pronounced for specimens impacted with the 12.7 mm impactor.

Figure 5 a) presents a comparison between the experimental curve and the numerical one at room temperature and Figure 5 b) presents the load-displacement curves obtained with the numerical simulations at room temperature and -150°C for specimens impacted with the 12.7 mm impactor and the 5 kg mass. The results of the simulations presented in this paper are preliminary, as energy problems are encountered and are mostly caused by element deletions and distortions. The preliminary results show that the model captures well the global behavior under impact at room temperature. The panel rigidity and the initiation of damage are well predicted. However, the numerical model slightly underestimates the maximum displacement. The latter might be caused by energy dissipation through artificial phenomena. The effect of temperature on the load-displacement curves is overall well captured by the model.

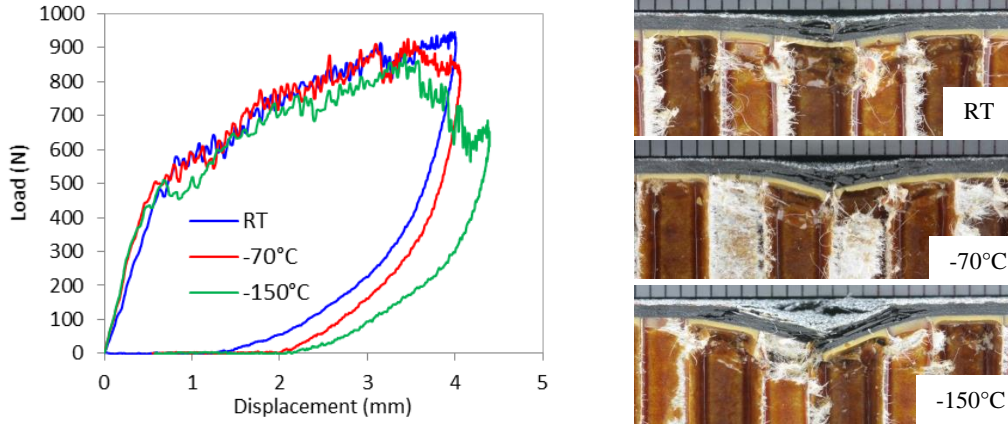


Figure 4. Load displacement curves and impact damage for specimens impacted with the 12.7 mm impactor and a 5 kg mass at room temperature, -70°C, and -150°C.

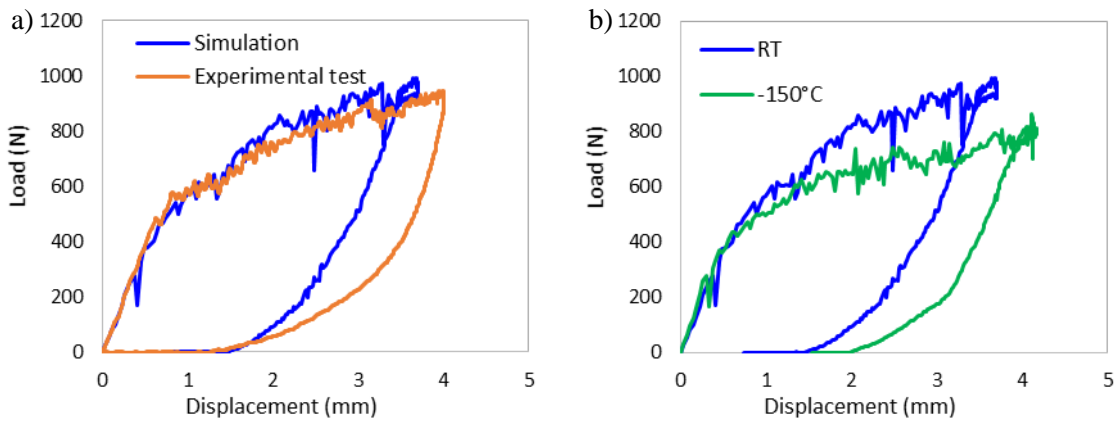


Figure 5. a) Experimental and numerical load-displacement curves at room temperature and b) numerical load-displacement curves at room temperature and -150°C for specimens impacted with the 12.7 mm impactor and a 5 kg mass.

## 6 CONCLUSION

The effect of extreme low temperatures on the low velocity impact behavior of composite sandwich panels was studied. Experimental impact tests were performed at room temperature, -70°C, and -150°C. The results show that impact loadings at cold temperatures induce a larger amount of damage on the composite sandwich specimens. This emphasizes the need for testing composite structures in extreme environments.

A numerical model is developed to reproduce impact loadings at different temperatures. The results of the model, although preliminary, are promising. The global behavior of the panel under impact is well predicted. The effect of temperature seems to be overall captured by the model. A lot of hypotheses were made for many of the properties used at cold temperatures. A larger number of experimental tests at cold temperatures for characterisation purposes will probably help improve the model. Overall, the results of the numerical simulations show that this type of model is well suited to reproduce the behavior of composite materials at extreme cold temperatures.

## 7 ACKNOWLEDGEMENTS

The authors fully acknowledge the supports from the National Sciences and Engineering Research Council of Canada and the Canadian Space Agency.

## REFERENCES

- Bažant Z.P. and Oh B.H. (1983). Crack band theory for fracture of concrete. *Mater Struct*, 16, 155–177.
- Brewer J.C. and Lagace P.A. (1988). Quadratic stress criterion for initiation of delamination. *J Compos Mater*, 22, 1141–1155.
- Donadon M. V., Iannucci L., Falzon B.G., Hodgkinson J.M. and de Almeida S.F.M. (2007). A progressive failure model for composite laminates subjected to low velocity impact damage. *Comput Struct*, 86, 1232–1252.
- Elamin M., Li B. and Tan K.T. (2018). Impact damage of composite sandwich structures in arctic condition. *Compos Struct*, 192, 422–433.
- Erickson M.D., Kallmeyer A.R. and Kellogg K.G. (2005). Effect of temperature on the low-velocity impact behavior of composite sandwich panels. *J Sandw Struct Mater*, 7, 245–264.
- Gauthier L. (2010) Modelling of high velocity impact on composite materials for airframe structures application. Thèse de Doctorat, Université laval.
- Gómez-del Río T., Zaera R. and Navarro C. (2003). Prediction of the effect of temperature on impact damage in carbon / epoxy laminates. *J Phys IV*, 110, 699–704.
- Gómez-del Río T., Zaera R., Barbero E. and Navarro C. (2005). Damage in CFRPs due to low velocity impact at low temperature. *Composites, Part B*, 36, 41–50.
- Hochard C., Aubourg P.A. and Charles J.P. (2001). Modelling of the mechanical behaviour of woven fabric CFRP laminates up to failure. *Compos Sci Technol*, 61, 221–230.
- Hou J.P., Petrinic N., Ruiz C. and Hallett S.R. (2000). Prediction of the effect of temperature on impact damage in carbon / epoxy laminates. *Compos Sci Technol*, 60, 273–281.
- Jean-St-Laurent M., Dano M-L. and Potvin M-J. (2018) Effect of extreme cold temperatures on the behaviour under low velocity impacts of composite sandwich panels for lunar exploration rovers. CASI ASTRO-18, Québec, Canada, 15-17 May 2018.
- Lapczyk I. and Hurtado J.A. (2007) Progressive damage modeling in fiber-reinforced materials. *Composites, Part A*, 38, 2333–2341.
- López-Puente J., Zaera R. and Navarro C. (2002). The effect of low temperatures on the intermediate and high velocity impact response of CFRPs. *Composites, Part B*, 33, 559–566.
- Sakly A., Laksimi A., Kebir H. and Benmedakhen S. (2016). Experimental and modelling study of low velocity impacts on composite sandwich structures for railway applications. *Eng Failure Anal*, 68, 22–31.
- Salehi-Khojin A., Mahinfalah M., Bashirzadeh R. and Freeman B. (2007). Temperature effects on Kevlar/hybrid and carbon fiber composite sandwiches under impact loading. *Compos Struct*, 78, 197–206.
- Sánchez-Sáez S., Barbero E. and Navarro C. (2006). Analysis of the dynamic flexural behaviour of composite beams at low temperature. *Compos Sci Technol*, 67, 2616–2632.
- Turon A., Dávila C.G., Camanho P.P. and Costa J. (2007) An engineering solution for mesh size effects in the simulation of delamination using cohesive zone models. *Eng Fract Mech*, 74, 1665–1682.
- Yang P., Shams S.S., Slay A., Brokate B. and Elhajjar R. (2015). Evaluation of temperature effects on low velocity impact damage in composite sandwich panels with polymeric foam cores. *Compos Struct*, 129, 213–223.
- Composite Materials Handbook Volume 2. Polymer matrix composites: Materials properties. SAE International, 2012.